Measurement of the Temperature Influence on the Current Distribution in Lithium-Ion Batteries

Sabine Paarmann,* Lisa Cloos, Jakob Technau, and Thomas Wetzel

Herein, a comprehensive experimental studies on the interdependence of temperature and current distribution in lithium-ion batteries is presented. Initially, a method for measuring the current distribution on a single cell is presented and verified by comparison with measurements on a parallel circuit. The presented method is straightforward and robust. It provides accurate quantitative and reproducible results. They are consistent with literature and show a higher current with increasing temperature. This temperature dependency is more pronounced at lower temperatures. Furthermore, it offers the opportunity to determine the influence of the temperature on the current distribution more precisely. Finally, this publication correlates the normalized current with temperature quantitatively using an Arrhenius-like approach according to $I \sim \exp\left(-\frac{1}{T}\right)$.

1. Introduction

Lithium-ion batteries are widely used for energy storage in various applications ranging from mobile phones to electric vehicles. Especially for the latter, the requirements for battery performance and durability are particularly high, even in addition to demanding operating and ambient conditions.[1] Therefore, scientific research focuses on improving the energy and power density as well as the lifetime of batteries. Along with numerous other factors, the temperature has a significant impact on the electrochemical processes within the cell and consequently on the overall cell performance and aging behavior.[2–4] According to the Law of Arrhenius,[5] reaction rates increase exponentially with increasing temperature. This behavior can be expressed by the exponential function[6] according to Equation (1), in which R is the internal cell resistance, A a pre-exponential factor, E_A the activation energy, R_m the molar gas constant, and T the temperature.

$$R = A \cdot \exp\left(\frac{E_A}{R_m \cdot T}\right) \tag{1}$$

In addition, the diffusion coefficients in the active materials and in the electrolyte increase with higher temperatures[7,8] and thus the internal resistance of the cell decreases. As the mentioned cell properties themselves affect the heat generation inside the cell during operation,[9,10] there is a strong interaction between electrical cell behavior and the internal cell temperature. Temperature inhomogeneities inside a battery can be measured with an instrumented cell with in situ measurement techniques during operation.[11–13] They can be induced by the inhomogeneous inner heat transfer paths and the anisotropic properties, caused by the layered structure of the electrode stacks,[14,15] with their typical combination of materials with high and low heat conductivity.[16] Furthermore, external conditions, such as the cooling system, can cause temperature inhomogeneities on the surface and within the cell.[17,18] Due to the aforementioned strong interaction of temperature, resistance and current, an inhomogeneous internal temperature distribution leads to an inhomogeneous current distribution.[19] This direct relationship between temperature and current distribution is critical for cell behavior and aging.[20,21]

Although there are clear reasons to attempt determining distributions of current and temperature within the cell, e.g., to better understand their interdependencies and effects on cell behavior, both are difficult to measure. There are approaches to measure the current distribution[22,23] and potential differences[24,25] in-situ with multi-tab cells. The results show a dependence on the open circuit voltage (OCV) and an increase in inhomogeneity with C-rate and temperature.[22,25] However, such in situ measurements are not possible without affecting the cell.[13,19] In general, a cell is a parallel connection of individual electrode sheets. Therefore, a parallel connection of several cells was proposed as an alternative to investigate the current distribution.[19] In a parallel connection of multiple cells, the overall current is divided among the individual cells.

Regarding temperature, there are both simulative[26–28] and experimental[27–29] investigations on its influence on the current distribution in parallel connected cells. The studies differ in terms of cell chemistry, number of cells, temperature differences, and temperature level, however, they achieve similar conclusions. As the temperature influences the resistance, different cell temperatures in a parallel connection lead to an inhomogeneous current distribution. The warmest cell has the highest current

S. Paarmann, L. Cloos, J. Technau, Prof. T. Wetzel
Institute of Thermal Process Engineering
KIT
Kaiserstr. 12, 76131 Karlsruhe, Germany
E-mail: sabine.paarmann@kit.edu

The ORCID identification number(s) for the author(s) of this article can be found under https://doi.org/10.1002/ente.202000862.

before charge compensation takes place. The higher the temperature difference, the higher is the inhomogeneity, especially at lower temperatures,[27–29] which is attributed to the Arrhenius relation of the resistance.[29] The warmer cell, which is initially discharged with a higher current, reaches a lower state of charge (SOC) earlier. The difference between the voltage and the OCV increases,[30] which leads later on during the discharge to a decreased current through the warmer cell and therefore to an increasing current in the coldest cell.[27] Thus, the current distribution is also influenced by the shape of the OCV-versus-SOC-function and the changes in its gradient, which affect the profiles of the individual cell currents.[26,29,31,32] In addition, after terminating charge or discharge processes, charge compensation between the cells takes place,[33,34] so that the differences in the OCV as a function of the SOC are neutralized.[35] Furthermore, the C-rate has an influence on the individual cell currents.[29,36]

Apart from temperature, even slight deviations among cell parameters, such as in the internal resistance[37] and capacity[26] cause an imbalanced distribution of the current. According to Wang et al.,[38] electrolyte diffusion polarization has the strongest contribution to an inhomogeneous current distribution in a module. In the long term, cell-to-cell variations in the current may induce inhomogeneous degradation,[19] which can be intensified by thermal inhomogeneities.[39] Baumann et al.[40] discussed different indications concerning the development of cell-to-cell variations over the number of cycles and conclude that aging leads to a divergence of the state of health of the cells. Shi et al.[41] confirmed that an inhomogeneous current distribution has an influence on the rate of capacity fade. Cavalheiro et al.[42] showed that an inhomogeneous temperature distribution leads to accelerated aging, such as capacity decrease and resistance increase, in their experimental setup of five cells in parallel.

In addition to the uneven aging behavior or other parameter variations among the cells in a parallel configuration, the test setup and the interconnection itself pose a further challenge.[34] Fill et al.[43] investigated the influence of the test bench and contact resistances on the current distribution. Unequal wiring and contacting of the cells has an influence on the current distribution.[34,44–46]

When using a parallel connection to measure the temperature dependency of the current, the presented problems always arise. Therefore, this work presents a) a method to measure the temperature dependency of the current distribution while avoiding the disadvantages of both the measurements on the parallel connection and the in situ measurements on a single cell and b) a quantitative correlation for the temperature dependency of the current distribution. For this purpose, a commercial cell is exposed to a previously recorded voltage curve at different externally imposed homogeneous temperatures and the resulting current under these conditions is measured. The results are compared with those from a parallel connection of three cells, in which both the influence of temperature difference and temperature level are considered. Subsequently, the findings are evaluated and discussed regarding the temperature dependency of the current distribution.

2. Experimental Section

For the comparability of both experimental methods, specifically the measurements on the parallel connection and those on the single cell, cells of the same cell type and from the same production batch were used. The cell specifications are shown in **Table 1**. The measurements were performed using two cell test devices, a BaSyTec CTS for the single cell tests and a BaSyTec XCTS, which can provide higher currents, for the parallel connection tests.

Well-defined thermal, electrical, and mechanical boundary conditions were applied with carefully designed cell holders. They ensured a precise temperature control at the surface and tabs of the cell, reliable, low resistance electrical contact as well as a constant mechanical pressure on the cells.[20] The cell holders comprised two temperature control plates, made of aluminum. These plates were equipped with internal channels for a heat transport fluid, that was temperature controlled by thermostats. The setups were carefully thermally insulated to exclude environmental influences. In addition to this direct control of thermal boundary conditions, the parallel connection setup with three cells at different temperatures was kept at a constant ambient temperature of 23 °C by placing it in a climate chamber. This temperature was chosen because current measurement devices are potentially influenced by temperature fluctuations and the power meter has an optimum operating temperature of 23 °C. The single cell setup was placed in a thermally insulated safety box. In both cases, the temperature was varied within the range of 0 to 50 °C.

Before starting the experiments, the cells were postformed with 30 charge/discharge cycles with C/5 and the OCV and impedance spectra were measured at a temperature of 25 °C. **Figure 1** shows (a) impedance spectra at 50 % SOC and (b) the OCV of these cells. While the OCV curves were almost identical, there were slight deviations in the impedance. The cells had the same history and were from the same manufacturing batch, so these deviations might be due to manufacturing uncertainties.[47]

2.1. Parallel Connection

The test rig with three cells electrically connected in parallel, is shown in **Figure 2**a, whereas Figure 2b shows the electrical wiring. The different coloring indicates the temperatures; the star symbols mark the temperature measuring points. The picture was taken during mounting and before any thermal insulation was attached. Each cell had an individual cell holder (1–3) that

Table 1. Specifications of the investigated Li-ion cell SLPB 8043140H5 from Kokam Co., Ltd.

Nominal capacity (data sheet)	3.2 Ah
Capacity measured at nominal conditions	3.0 Ah
Nominal voltage	3.7 V
Voltage range $U_{min}-U_{max}$	2.7–4.2 V
Anode material	Graphite
Cathode material	NCA/LCO
Cell attributes	Pouch cell
	High-power cell
	Opposing tabs

2000862 (2 of 11)
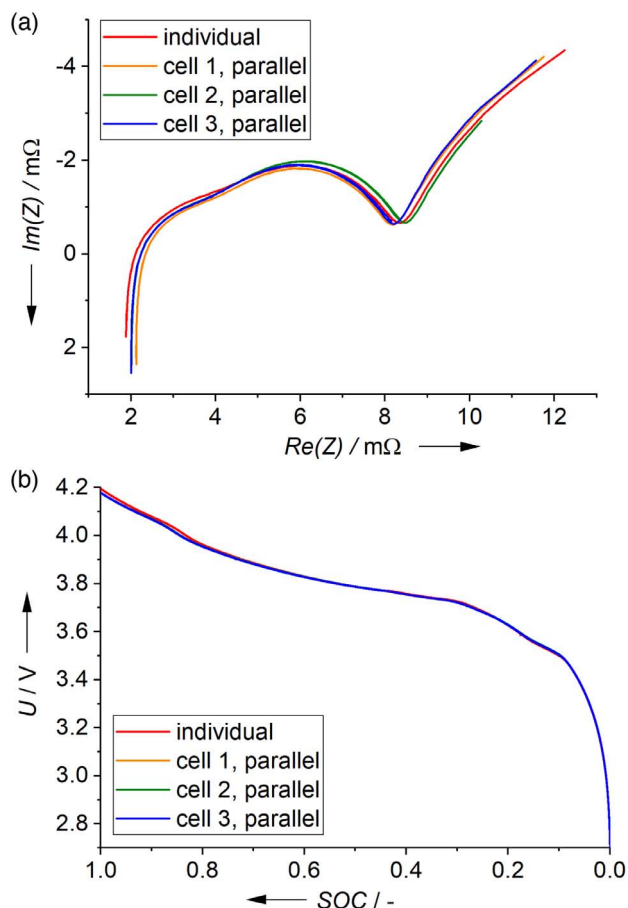
Figure 1. a) Impedance spectra at 50% SOC and b) the OCV of the four cells used for the measurements.

identical cells according to the previous formation were selected for the parallel circuit. The cells were randomly assigned to the cell holders without consideration of the future temperature level. **Table 2** presents the test matrix for the temperatures at which the experiments were performed. The influence of the temperature level was observed by varying the mean temperature T_M of the parallel connection with a temperature difference of 25 K. For the mean temperature T_M of 25 °C, the influence of the maximum temperature differences ΔT was studied, which was varied from 0 to 50 K. This determines the temperatures for the cells, which are noted in columns 3–5.

As the focus of this study is on the influence of temperature, a fixed C-rate of C/2 was applied. This corresponds to a current of 4.5 A for the parallel connection of three single cells. During the experiments, the measured temperature at the electrode stack
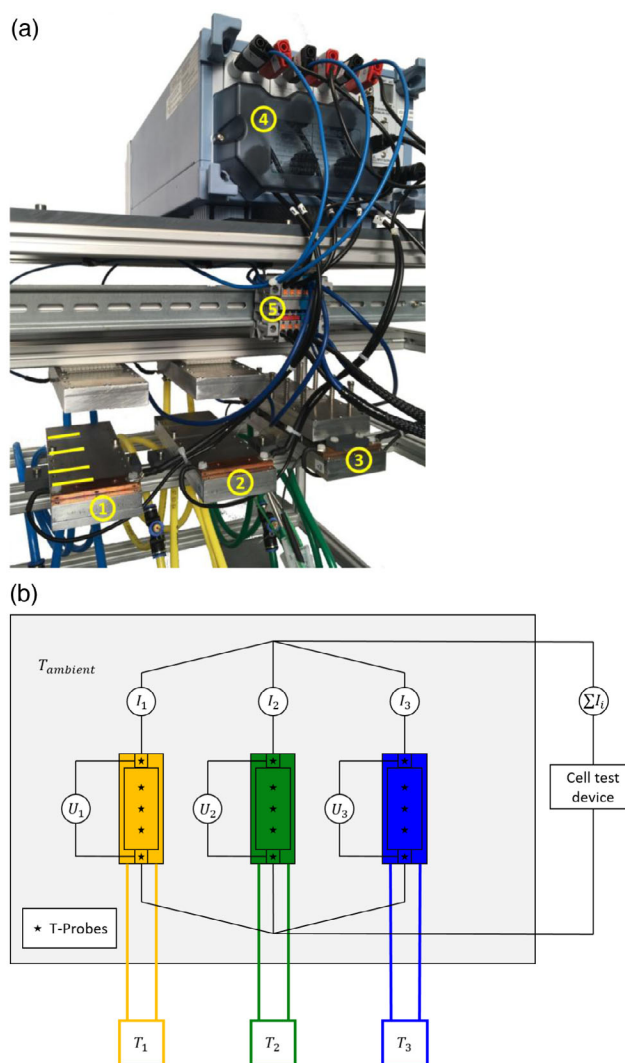
was supplied separately by thermostats with a fluid flow at a constant temperature through different colored hoses. In cell holder (3), the cell was already mounted and clamped between the temperature control plates. At the upper plate, spring screws for constant mechanical pressure are visible. The other two holders are still vacant, with the upper plates lifted. In the lower plates, notches for surface temperature measurement with thermocouples are visible. Further thermocouples were located in the fluid supply lines to the plates. The total current of the parallel connection was specified via the cell test device, whereas the current, voltage, and charge throughput of the individual cells were measured by a separate power meter from Yokogawa Denki K.K (model WT333E) (4). At the node (5), the current was split between the cells. During the assembly, exactly the same and shortest possible wiring was used for all cells to avoid any influence of the setup. The electrical contacting was realized via a copper strip where the tabs were pressed and the cables brazed onto to reduce contact resistances. The testing procedure was performed automatically via a LabVIEW control running on a PC, connected via USB or ethernet to the cell test and measurement devices and the thermostats.

As previously discussed, even small differences in the cell characteristics have an effect on the current distribution, so the cell selection is important.[37,48] Therefore, the three most

Figure 2. a) Test setup for a parallel connection with three cell holders (1–3) with individual temperature control plates, the power meter (4) to measure the cell currents originating from the node (5) where the current is splitted. b) Schematic illustration of the electrical wiring with colored highlighting of the different temperatures and star symbols marking the temperature measuring points.

Table 2. Test matrix for the experiments on the parallel connection including the mean temperature, the maximum temperature difference, and the temperatures of the individual cells.

Mean temperature T_M [°C]	Temperature difference ΔT [K]	Temperature Cell 1 [°C]	Temperature Cell 2 [°C]	Temperature Cell 3 [°C]
25	0	25	25	25
	10	30	25	20
	20	35	25	15
	25	37.5	25	12.5
	30	40	25	10
	40	45	25	5
	50	50	25	0
12.5	25	25	12.5	0
37.5	25	50	37.5	25

deviated by a maximum of 2% from the set temperature. The largest deviations of 2 K from the set point temperature occurred at low temperatures at the cathode tab, as both the heat generation by the current and the parasitic heat transfer from the environment are at their maximum in this case. The core temperature of the cell is impossible to quantify in this setup, but it is known from previous experiments, that heat generation at low C-rates is low for this cell.

The testing procedure followed the flow chart in **Figure 3**a. First of all, the parallel connection was fully charged via a constant current–constant voltage charge protocol with a cut-off current of C/20 and at a temperature of 25 °C. At the same temperature, the cell was fully discharged with C/2. The results for the current distribution of this discharge are used later on in Section 3.1 as a reference discharge. Based on a complete discharge starting again at SOC of 100%, the discharge behavior is analyzed.

2.2. Individual Cell

To measure the current as a function of temperature on an individual cell, any current control within the setup must be avoided. This is being realized in the present experiments by first measuring a discharge curve at a constant current on the postformed cells. Subsequently, this voltage curve was used to control the voltage with the "Table" command in the BaSyTec software. A data table which contains voltage values for each point in time of the previously recorded discharge is used as load profile. During each discharge, a different temperature was applied onto the cell. The test procedure for the individual cell is likewise shown in Figure 3b. The boxes shaded in gray indicate the steps that are performed only once and which serve to record the voltage curve. The voltage curves were recorded with a constant current of C/2 (1.5 A) starting from 100% SOC and at different temperatures T which have been kept constant at 12.5, 25, and 37.5 °C, respectively. The recorded voltage curves are shown in **Figure 4**. Whenever we mention the "recorded voltage" in this publication, these voltage curves are referred to.

Each current measurement started with a constant current (CC)–constant voltage (CV) charging procedure with a cut-off current of C/20 and at a temperature of 25 °C as indicated by the first white box in Figure 3b. Then the temperature was first stabilized at the desired value before the battery was (dis-)charged with a current of C/20 to the voltage U_{Start} at which the target voltage curve starts. This procedure was necessary, as the OCV changes with temperature. As a result, high current peaks at the beginning of the measurement were avoided. This also means the SOC is not exactly the same at the beginning of each measurement. Therefore, the initial condition corresponds to that of the single cells in the parallel connection, when the temperature is individually controlled.

The current measurements for investigating the temperature influence were then carried out by specifying each of the determined voltage curves at constant homogeneous temperatures in
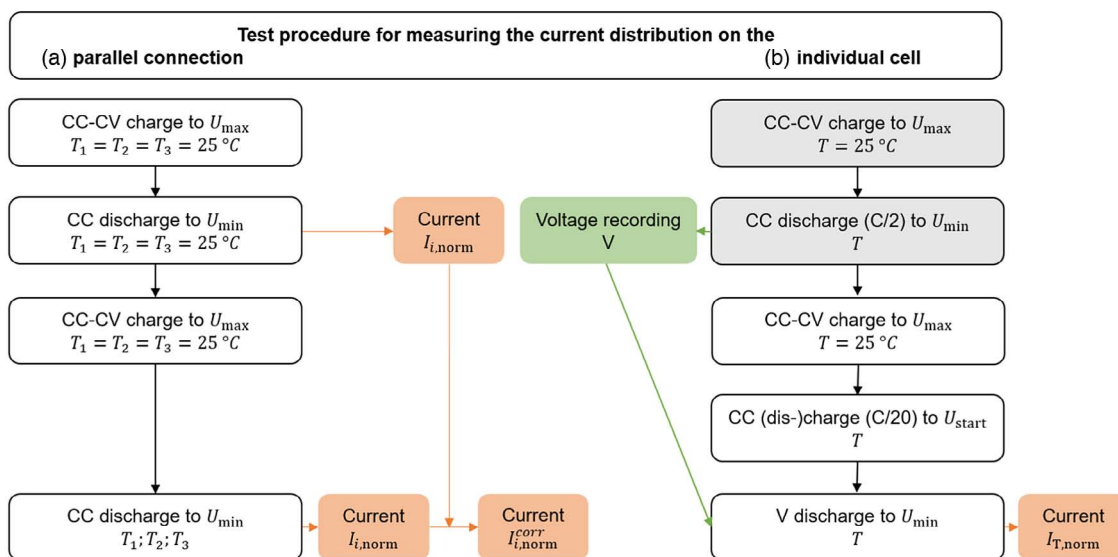

Figure 3. Flow chart with the testing procedure for a) the parallel connection and b) the individual cell. The boxes shaded in gray indicate steps that are only performed once; the orange boxes indicate the results for the current distribution.
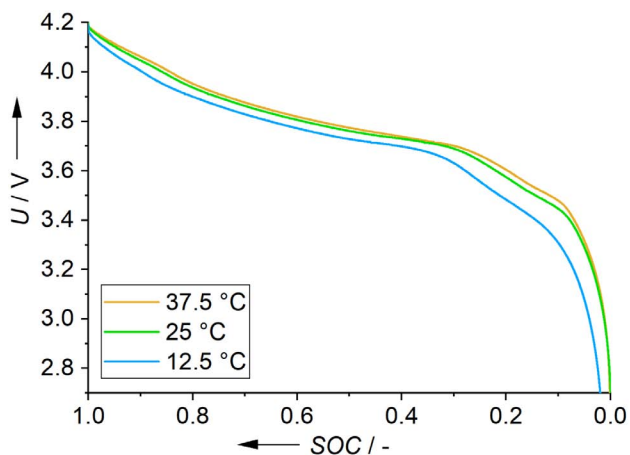
Figure 4. Recorded voltage curves of the future voltage specifications resulting from different temperatures and a constant current of C/2.

Table 3. Test matrix for the experiments on the individual cell including the temperature during the voltage recording and the temperatures that were applied to the individual cells during the current measurements while the voltage was controlled.

Temperature during voltage recording [°C]	12.5			25						37.5		
Temperatures during current measurement [°C]	0	12.5	25	0	5	10	12.5	15	25	0	12.5	25
	37.5	50	30	35	37.5	40	45	50	–	37.5	50	

the range of 0 to 50 °C. **Table 3** presents in the first line the three temperatures at which the voltage was recorded and in the second line the temperatures for which these voltages where applied to the cell, respectively.

3. Results and Discussion

In the following, the results of the current distribution in the parallel connection and the individual cell are presented and discussed. These findings are then compared to each other and a quantitative correlation between current distribution and temperature is derived.

3.1. Parallel Connection

The current distribution is expressed by the normalized current $I_{i,norm}$ for each cell i. It is defined according to Equation (2) as the cell current I_i divided by the average current of the cells within the parallel connection which is one-third of the total constant current, in this case 1.5 A. For an ideal current distribution among the three cells, the normalized current of each cell would be 1. The normalized current is plotted against the SOC of the parallel connection.

$$I_{i,norm} = \frac{3 \cdot I_i}{\sum_{i=1}^{3} I_i} \tag{2}$$

In the following, first the influence of temperature is described before the differences in the current curves of the three cells are discussed. The temperature effect on the current distribution between the cells is presented and discussed in the following using the examples of 5, 25, and 45 °C as cell temperatures. This represents a mean temperature T_M of 25 °C and a maximum temperature difference ΔT of 40 K. Overall, the curves shown in **Figure 5**b have the same shape compared to the uniform temperature at 25 °C in Figure 5a. But as expected, the current curves differ to a greater extent. At the end of discharge, when the voltage curve becomes steeper, the differences are more prominent. There the deviations in the SOC, which have built up during the course of the discharge are increasingly compensated. The following statements are with regard to the plateau phase, as it ensures the best basis for comparison. The temperature level affects the position relative to the y-axis. The lower temperature of 5 °C reduces the current of cell 3 (blue) significantly, whereas the current of cell 1 (orange) increases due to the higher temperature of 45 °C. Compared to cell 2 (green) at 25 °C, it still has a lower current which is unexpected in comparison to the results from Yang et al.[27,28] and Klein and Park.[29] But it can be attributed to the different cell characteristics. It is noteworthy,
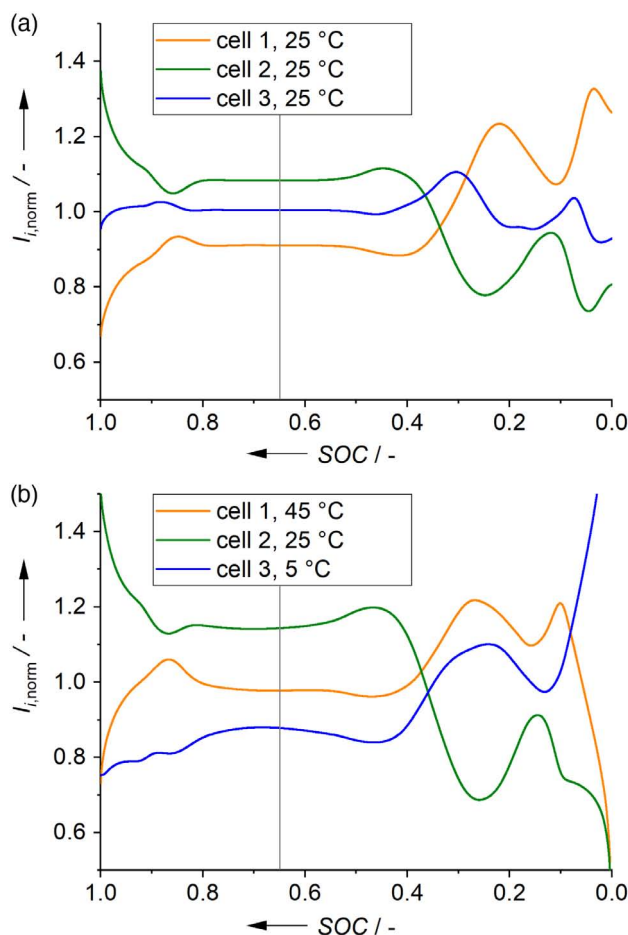

Figure 5. Normalized current against the SOC of the parallel connection at a mean temperature of 25 °C for a) a uniform temperature of 25 °C and b) a maximum temperature difference of 40 K.

however, that first cell 2, which has the mean temperature of 25 °C, is also exposed to a higher current compared with the homogeneous case and second that despite the same temperature difference, the current decrease from cell 3 at 5 °C is larger than the current increase from cell 1 at 45 °C. This means that a symmetrical temperature distribution does not necessarily lead to a symmetrical current distribution, which was also seen by Klein and Park.[29] In their case, the effect differed for different cell chemistries. The LFP cells were much more symmetrical compared with NMC cells, which was attributed to a more linear temperature dependency.

The normalized current curves of the three cells for a discharge are significantly different even at a uniform temperature as shown in Figure 5a for a temperature of 25 °C. Similar results are obtained at lower and higher uniform temperatures. In general, the characteristics of the individual current curves and their distribution agree well with observations made by the other authors mentioned earlier and can be explained by differences in resistance and capacity of the individual cells. These impedance and capacity variations which are not high but still visible in Figure 1 can explain the current difference.[26,37] Another challenge concerning the reproducibility is the sensitivity of the system. The results obtained appeared susceptible to irregularities such as longer downtimes and operation at cold temperatures such as 0 and 5 °C. This results in voltage and current fluctuations during the discharge. Voltage fluctuations are also seen by

Lv et al.[44] and deviating results can be attributed to this. This is possibly aggravated by the previously outlined aging in parallel connections. These differences are significant because their influence is of the same order of magnitude as the temperature influence, which can be derived from the deviations of the normalized current from 1 in Figure 5.

The strong impact of the cell properties on the current distribution impedes a clear evaluation of the temperature effects. Therefore, a reference or baseline case in which all cells have a temperature of 25 °C is introduced.

In the ideal case, if the cells were perfectly equal, the normalized current would be 1 for every cell at a uniform temperature. As shown earlier, the temperature difference shifts the currents compared to a uniform temperature. To extract this temperature influence, the difference between the ideal and real current distribution at a homogeneous temperature must be ground off. At 65 % SOC, the deviation from the ideal case in which the normalized current equals 1 is evaluated for each cell and, with the assumption that the temperature influence on the current distribution is independent of the SOC, the individual normalized current curves are shifted entirely in y-direction. The SOC of 65% was selected because it lies within the operating window of hybrid vehicles[1] and because of its position on the plateau where the current distribution is stable and not as susceptible to external factors. The corrected normalized current is calculated using Equation (3). **Figure 6**a shows the effects of the correction when
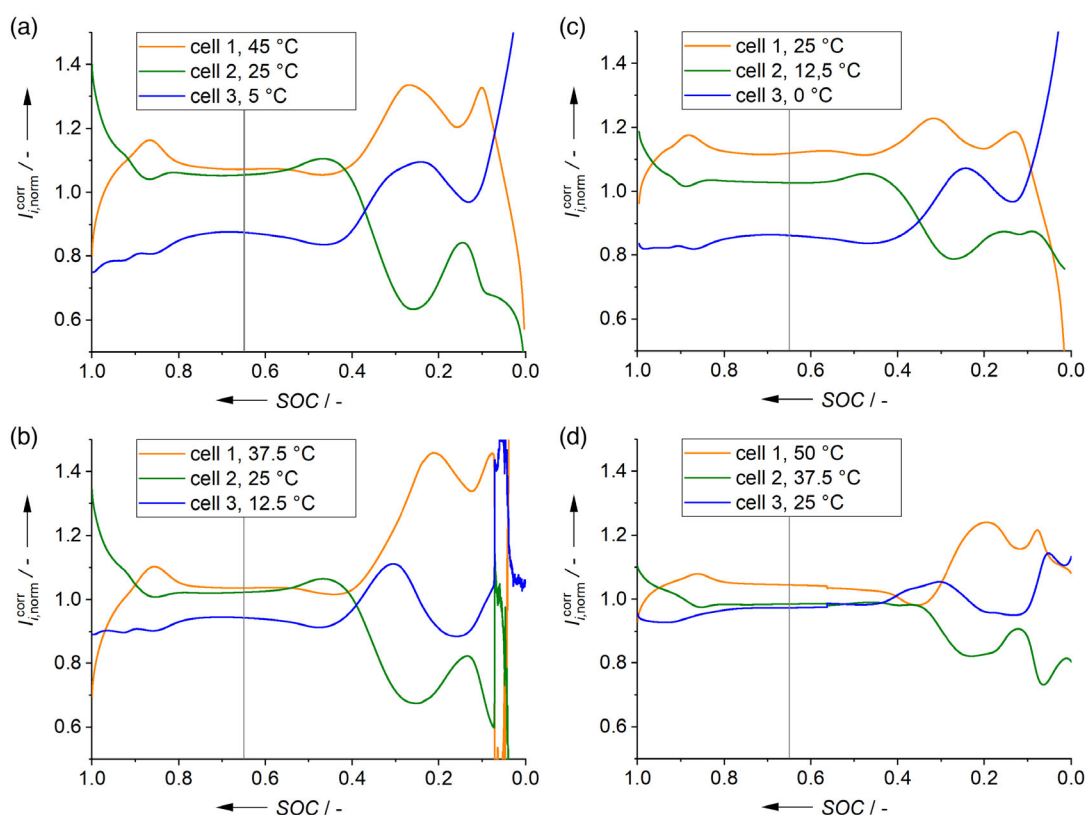

Figure 6. Normalized current against the SOC of the parallel connection at a mean temperature of 25 °C and a maximum temperature difference of a) 40 K and b) 25 K as well as the normalized current at a mean temperature of c) 12.5 °C and d) 37.5 °C both with a maximum temperature difference of 25 K.

**ADVANCED
SCIENCE NEWS**
www.advancedsciencenews.com

Energy Technology
Generation, Conversion, Storage, Distribution
www.entechnol.de

compared with Figure 5b. The blue curve (cell 3) with its plateau at about 1 in the reference case (Figure 5a) is not affected by the correction. In contrast, the orange curve of cell 1, which was below 1 in the reference case, is shifted upward while the green curve of cell 2 is shifted downward. Even then, the curves for cell 2 and cell 3 are very close to each other.

$$I_{i,\text{norm}}^{\text{corr}} = \frac{I_{i,\text{norm}}}{I_{i,\text{norm}}(\text{SOC} = 65\%, T_i = 25\,^\circ\text{C})} \tag{3}$$

The results for the temperature difference of 40 K are shown in Figure 6a and directly compared with the temperature difference of 25 K, Figure 6b. The results reveal a broader distribution of current when the maximum temperature difference is increased while keeping the mean temperature constant. This is consistent with the results of other authors on parallel connections of lithium-ion batteries.[27,29] In addition to the temperature difference, the temperature level has a decisive impact. This influence is shown in Figure 6b–d based on the current distribution at a maximum temperature difference of 25 K and mean temperatures of 25, 12.5, and 37.5 °C, respectively. As the mean temperature decreases, the current distribution diverges, which is also as expected.[28,29] At the mean temperature of 12.5 °C, the current of the coldest cell (0 °C) is significantly lower than the current of the other two cells, nevertheless, their difference is also greater than at higher temperatures.

The evaluation of the current distribution by depicting the normalized current during the whole discharge process is well established in the literature. To compare a multitude of results with each other, the current distribution is evaluated at 65% SOC. **Figure 7** shows this current for the different experiments as a function of the maximum temperature difference. The experiments were repeated several times and the mean value and standard deviation were calculated for each temperature. The mean values are plotted in the diagram and the error bars depict the standard deviation.

Figure 7 shows the normalized current for a mean temperature of 25 °C over the maximum temperature difference between the warm and cold cell. The temperature distribution was symmetrical, so cell 2 was always at the mean temperature of 25 °C.
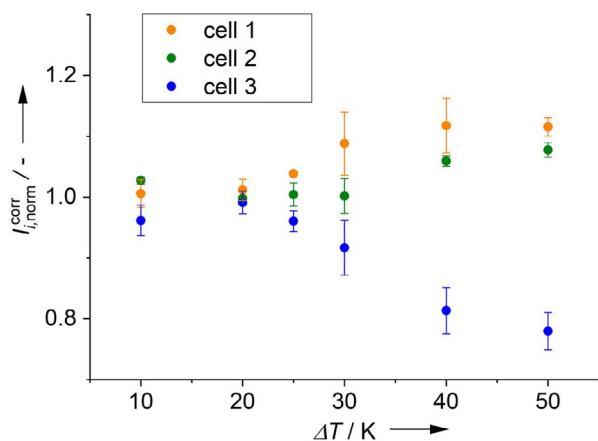

Figure 7. Normalized cell current for different maximum temperature differences with a mean temperature of 25 °C.

According to this, a temperature difference below 30 K has hardly any effect on the current distribution. With increasing temperature difference, the differences in current increase. This is especially true for the current of the coldest cell which declines rapidly, while the currents of the warmest cell and the cell at 25 °C do not differ that strongly.

It can be concluded that the temperature influence on the current distribution is not linear. First, this can be seen in the unsymmetrical current distribution at high symmetrical temperature differences in Figure 7. Second, the current differences increase with lower average temperature but the same temperature differences as shown in Figure 6.

3.2. Individual Cell

The evaluation of the current in the individual cell experiments is likewise realized via the normalized current calculated by Equation (4). The reference value in this case is the current that was applied to record the voltage curve, which is C/2 (1.5 A).

$$I_{\text{T,norm}} = \frac{I_{\text{T}}}{I_{\text{const}}} = \frac{I_{\text{T}}}{1.5\,\text{A}} \tag{4}$$

In the following diagrams, the normalized current for different temperatures is plotted over the SOC. Overall, it is apparent that the results in **Figure 8** are extremely similar to those of the parallel connection. After a short initial phase, a plateau is reached during which the current curves are fairly constant and parallel to each other. Toward the end of the discharge, a wavy pattern develops and the order is reversed. This can be attributed to the shape of the OCV and the difference that accumulates between cell voltage and OCV during the discharge,[30] which is larger for low temperatures. The temperature dependence of the normalized current is analog to the results of the parallel connection, but is revealed more clearly. When specifying the voltage from a discharge at 25 °C, the cell exhibits a significantly lower current for lower temperatures than for higher temperatures. At a temperature of 0 °C (purple), the cell draws the lowest current, whereas the current is highest at 50 °C (pink). The current curves at all in-between temperatures are perfectly in order of the temperature up to the end of the plateau phase. Furthermore, the distance between the curves indicates the influence of the temperature level. During the plateau, the largest distances between 0 °C/5 °C and 5 °C/10 °C are observed. This means that at a lower temperature level, the same temperature difference has a higher impact on the current. This indicates a higher temperature dependence at low temperatures. At higher temperatures, the differences in current decrease until the curves can hardly be distinguished above 35 °C. This behavior is identical when other voltage curves are specified as in Figure 8a–c and is consistent with the results of the parallel connection.

Comparing the shape of the current curve at different voltage specifications, none of the normalized current values in the plateau phase for the voltage recorded at 37.5 °C is found to be greater than 1. The plateau phase lasts longer up to lower SOC and the wavelike shape is much less pronounced than with the voltage specification measured at a temperature of 12.5 °C. In addition, the cell current at 0 °C is slightly lower
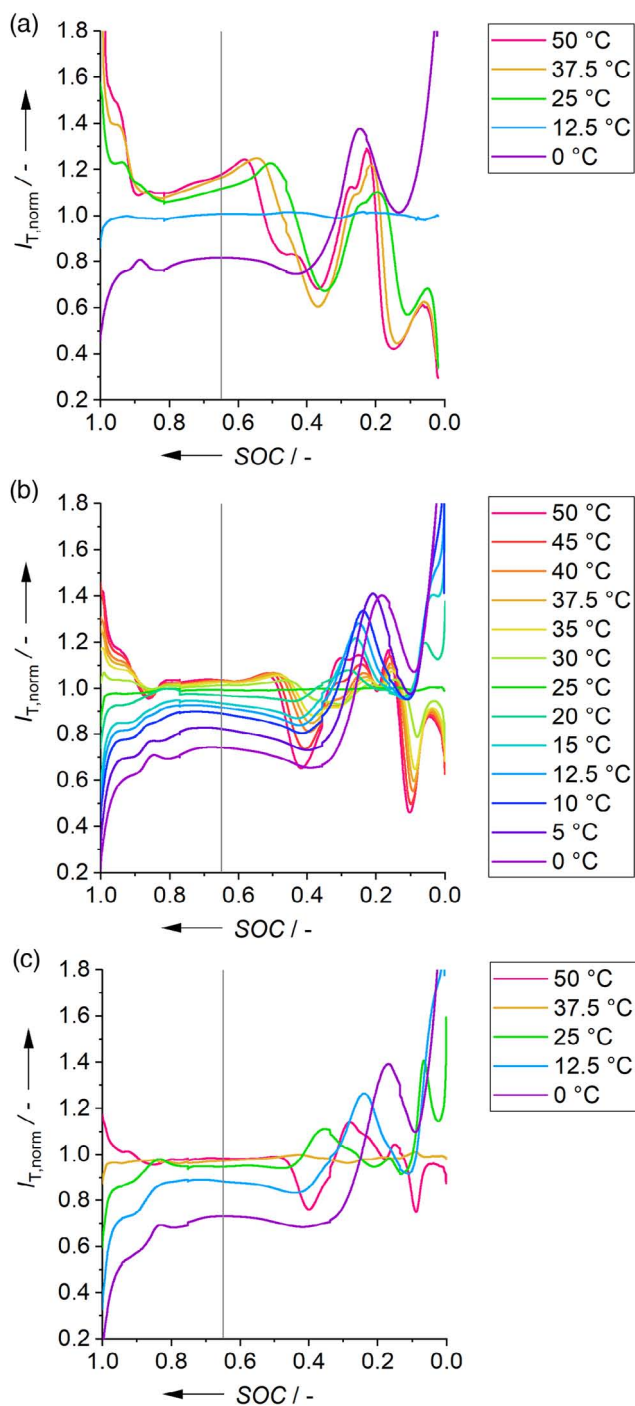
ADVANCED
SCIENCE NEWS
www.advancedsciencenews.com

Energy Technology
Generation, Conversion, Storage, Distribution
www.entechnol.de

Figure 8. Normalized current of the individual cell plotted against the SOC of the discharge during the voltage recording and at the temperature of a) 12.5 °C, b) 25 °C, and c) 37.5 °C, respectively.

in the plateau for the voltage specification at low temperatures, but rises considerably steeper at the very end of the discharge. This means that the cell voltage is far from the OCV, as the temperature affects the voltage and the overvoltage significantly. The temperature during voltage recording therefore has an influence on the current distribution to the extent that the current curves

measured at similar temperatures are closer to 1, as voltage, temperature, and current are related and the cell is close to a balanced state.

Furthermore, the normalized current at the temperature at which the respective voltage curve was measured, results in a virtually constant value of 1. In addition to the qualitatively good results, these cross-check measurements qualify this approach for measuring an equivalent current distribution on an individual cell. Compared to a parallel connection or an in situ measurement, this method has the advantage of a much simpler experimental setup, which is less susceptible to nonsystematic effects. Present measurement data are scarcely influenced by previous experiments and, most importantly, the results for the current distribution are not influenced by cell-to-cell variations, as the current is always measured on the same cell. In addition, for parallel circuit measurements, the temperature difference to the other cells in the circuit must always be considered and thus one cell or temperature level cannot be evaluated independently of the others. In contrast, the results of an individual cell can be clearly related to one temperature.

3.3. Comparison and Quantification of the Temperature Dependency

In this section, the temperature dependency of the normalized current measured on the individual cell is compared with the one in the parallel connection. In a second step, this dependency is quantified and described mathematically.

To explicitly illustrate the temperature dependency, the normalized current is plotted in **Figure 9** over the temperature. The green markers in (a) are the same data of the parallel connection as in Figure 7. The normalized current was evaluated at an SOC of 65% of the parallel connection for an average temperature of 25 °C. The inclination at low temperatures is steeper and flattens out with increasing temperature. The blue and orange markers represent the data for mean temperatures of 12.5 and 37.5 °C, respectively. In comparison, a higher mean temperature shifts the normalized current downward on the y-axis, whereas the lower mean temperature shifts the curve upward. The gradient of the normalized current corresponds to the one at the mean temperature of 25 °C in the respective temperature range. From previous experiments, it is known that the internal self-heating is relatively low for these cells at 25 °C and a C-rate of C/2, but it cannot be quantified with the results presented here. In the low temperature range, the internal resistance is higher and therefore the effect of internal self-heating is more relevant. This means that the curve for the temperature dependency would be even steeper at low temperatures without the effect of self-heating.

For the individual cell, the normalized current depends on the temperature at which the voltage profile was recorded. This dependence is evaluated in Figure 9b. Therefore, the normalized current was evaluated again at 65% SOC. In the case of the individual cell, the 65% SOC was defined based at the point in time when it was reached in the discharge during voltage recording. This is necessary because the V-discharge does not start at 100% SOC as indicated in Figure 3. This means that the current is evaluated at the same point in time regarding the voltage
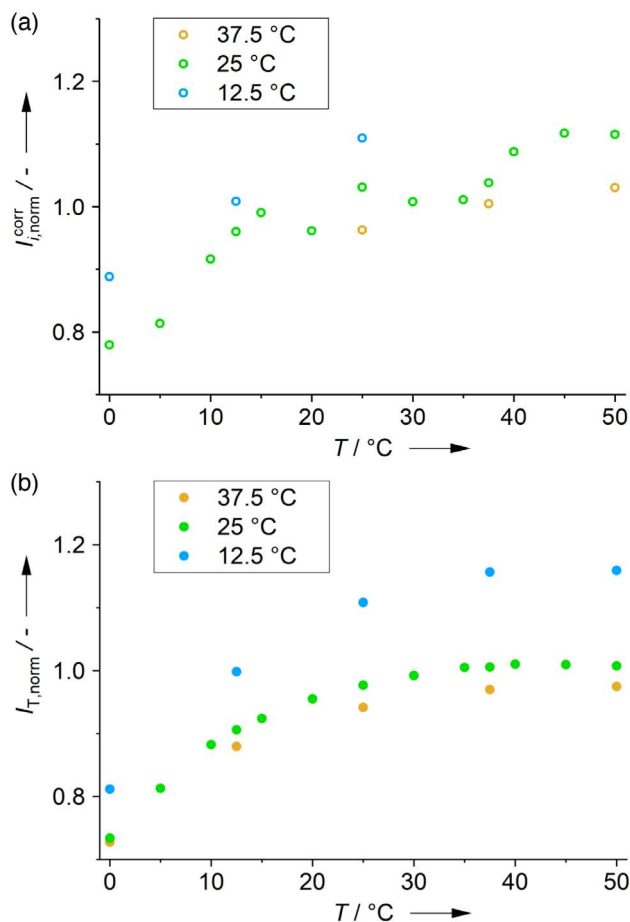
(a)

(b)

Figure 9. Normalized current of a) the parallel connection for different mean temperatures and of b) the individual cell for different temperature during voltage recording plotted against the temperature of the cell(s) during the discharge.

specification, but when measuring the current, the cell has a different SOC at different temperatures at this point. This way, it is comparable to the values obtained from the parallel connection. The normalized current was then plotted for all experiments as a function of the respective temperature. The markers in Figure 9 are of the same color for the test series in which the same voltage curve was applied at different temperatures. The advantage here is that the temperature during voltage recording is independent of the temperature at which it is specified for the current measurement. Therefore, the measurements can be easily extended to the whole temperature range. Consistently and in accordance with the measurement on the parallel connection, the incline of all plots is steeper at low temperatures, then flattens out with increasing temperature. A temperature increase above 35 °C only has a minor effect on the magnitude of the normalized current. Apart from these similarities, the curves have a different position relative to the *y*-axis. The lower the temperature level during the voltage recording, the higher the current during the discharge with voltage control for the same temperature. For instance, the normalized current at 37.5 °C has a value of 1.156 when a voltage is specified that was recorded at 12.5 °C (blue). It is higher

by 0.196 than the normalized current when a voltage is specified that was recorded at 37.5 °C (orange). Overall, the temperature dependency is similar to the one in the parallel connection. The results of both methods indicate the same dependencies of the normalized current on the temperature. Where the current is permitted as a degree of freedom by predefining the voltage curve, it adjusts according to the temperature. Thus, the current of a single cell shows the same temperature dependence as the one in a parallel connection. Purely qualitatively speaking, the normalized current increases with rising temperature, but this dependency diminishes at high temperatures.

Based on the previously introduced diagrams that depict the current versus temperature, a quantitative evaluation is now proposed. According to Ohm's law, the current is reciprocally proportional to the internal cell resistance. Simultaneously, the temperature dependence of the internal cell resistance follows an exponential function of the inverse temperature $R \sim \exp\left(\frac{1}{T}\right)$. Combining these two dependencies, the current distribution follows an Arrhenius-type function, as represented in Equation (5), where a, b, and c are constant coefficients. They are fitted with a nonlinear least-square solver to the measurement data for each measurement sequence. The Kelvin temperature is commonly used for Arrhenius approaches; therefore, this is chosen for the following evaluation as well.

$$I = a \cdot \exp\left(-\frac{b}{T - c}\right) \qquad (5)$$

In **Figure 10**, the measured values for the normalized current are given as markers over the temperature. The markers for the parallel connection are circles and those for the individual cell are filled. The lines represent the respective fits (dashed for the parallel connection) and are in good accordance with the measurement results, which is confirmed by the values for the coefficient of determination R^2 in **Table 4**. The table also includes the coefficients a, b, and c of Equation (5) that themselves exhibit a trend in their temperature dependency.

First, the results for the single cell are compared with regard to the temperature during the voltage recording. The coefficient a decreases with increasing temperature during voltage recording. This mainly affects the limit value to which the function converges. It is clearly visible in the diagram that this value is indeed lower at higher temperatures. Thereby, the already discussed dependency of the current distribution on the temperature at which the voltage was recorded is evident again. With a higher temperature during voltage recording, less overvoltages arise. This results in a flatter voltage curve and accordingly in a lower normalized current. The largest deviations arise for the parallel connection, which is apparent both in the graphical representation and in R^2. When comparing the data of the parallel connection at an average temperature of 25 °C with those of the single cell, where the voltage was recorded at 25 °C, discrepancies have to be noticed. The normalized current for the individual cell is slightly lower over the entire temperature range. This can be explained by the fact that lower temperatures have a strong effect on the normalized current and that the mean value of the evaluated data points at 65% SOC is with 0.94 clearly below 1. In contrast, when measuring on the parallel connection, the normalized currents at different temperatures are not
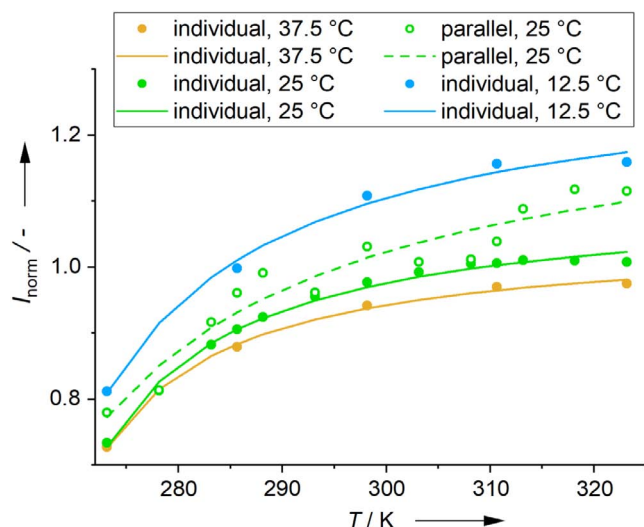
Figure 10. Normalized current of the parallel connection at a mean temperature of 25 °C and of the individual cell for different temperatures during voltage recording plotted against the temperature of the cell(s) during the discharge. The dashed lines are the fits of the exponential function for the respective data.

Table 4. Coefficients for the exponential fits for the different measurement series and its coefficient of determination R^2. The right-hand side column gives the mean value of the normalized current.

		a [–]	b [K]	c [K]	R^2	$\bar{I}_{norm}$ [–]
Individual cell	$T = 12.5\,°C$	1.308	6.975	258.6	0.9922	1.047
	$T = 25\,°C$	1.106	4.786	261.7	0.9921	0.940
	$T = 37.5\,°C$	1.048	4.009	262.2	0.9976	0.899
Parallel connection	$T_M = 12.5\,°C$	–	–	–	–	1.002
	$T_M = 25\,°C$	1.274	10.47	252.2	0.9089	0.987
	$T_M = 37.5\,°C$	–	–	–	–	0.999

independent on each other. The total current must be divided among the cells at any time. Thus the closing condition applies, according to which the mean value of the normalized current $\bar{I}_{norm}$ must be 1. The numbers for the mean values of the normalized current are listed in Table 4, both for the parallel connection for which they are very close to 1 and for the measurements on the individual cell. The results suggest that the temperature influence is revealed more clearly with the measurements on the individual cell, as they are independent on each other.

A further effect of this phenomenon is, that for the parallel connection, the curvature of the exponential function is less pronounced. This can be seen in the coefficient b in the exponent. The smaller this parameter is, the stronger is the curvature of the exponential function. For the measurements at the single cell, coefficient b increases with decreasing temperature during the voltage recording and is greatest for the parallel connection. The opposite applies to the coefficient c, which increases with

increasing temperature and has the lowest value for the parallel connection. Coefficient c is necessary for the fitting and shifts the curve on the x-axis, which makes it relevant for the use of the Kelvin temperature scale. A quantitative conclusion for the parallel connection about the dependency of the normalized current of the mean temperature using a fit is not feasible because the temperature range is too limited to adapt a reasonable function.

All in all, it can be concluded that a relatively simple function quantifies the temperature dependency of the normalized current distribution. However, it must be mentioned that an extrapolation to low temperatures below $-10\,°C$ is not applicable.

4. Conclusion

This work presents a new method to determine the current distribution as a function of temperature, using measurements on a single cell. The procedure leads to a significant improvement in terms of reproducibility and is simpler to handle than a parallel connection, which has been proposed so far in literature. The effect of temperature on the current distribution can be determined independently of the influence of the electrical connection, different cell parameters due to, e.g., manufacture and other stochastic effects. In addition, a correction method is presented, which takes these influences into account, when measuring parallel connected cells, so that the temperature influence can be isolated. With both options, a distinct temperature dependency could be shown, that is in line with former literature findings. Qualitative observations show that the current increases with increasing temperature, especially at low temperatures, while the temperature dependency is less pronounced at a higher temperature level. A quantitative evaluation reveals that an Arrhenius-type function can be found, that consistently correlates to all experiments in this publication, using temperature dependent coefficients.

For a transfer of the results to a cell discharged under an inhomogeneous temperature condition, the results derived from the parallel connection method might be more suitable, as the closing condition for the normalized current applies in both cases. On the other hand, the results suggest that due to the strong interactions of the cell currents in the parallel connection, the temperature of one cell also affects the behavior of the others and thus no plain and absolute temperature dependency of the current can be determined. This is possible with the experiments on the individual cell. Therefore, the results can very well be implemented into a coupled electrical-thermal simulation, where the electrical model considers effects of SOC and current distribution.

The approach to measure an equivalent current distribution on individual cells might be extended to study the influence of differing cell parameters. In this case, various cells with given parameters could be analyzed with the same voltage curve and the measured current could be correlated directly with these cell parameters without the influence of the interconnection.

Acknowledgements

Conflict of Interest

The authors declare no conflict of interest.

Keywords

[1] B. Ketterer, U. Karl, D. Möst, S. Ulrich, FZKA 7503, Karlsruhe **2010**.

[2] T. M. Bandhauer, S. Garimella, T. F. Fuller, *J. Electrochem. Soc.* **2011**, *158*, R1.

[3] I. Bloom, B. W. Cole, J. J. Sohn, S. A. Jones, E. G. Polzin, V. S. Battaglia, G. L. Henriksen, C. Motloch, R. Richardson, T. Unkelhaeuser, D. Ingersoll, H. L. Case, *J. Power Sources* **2001**, *101*, 238.

[4] J. Vetter, P. Novák, M. R. Wagner, C. Veit, K.-C. Möller, J. O. Besenhard, M. Winter, M. Wohlfahrt-Mehrens, C. Vogler, A. Hammouche, *J. Power Sources* **2005**, *147*, 269.

[5] S. Arrhenius, *Z. Physik. Chem.* **1889**, *4*, 226.

[6] J. P. Schmidt, S. Arnold, A. Loges, D. Werner, T. Wetzel, E. Ivers-Tiffée, *J. Power Sources* **2013**, *243*, 110.

[7] T. L. Kulova, A. M. Skundin, E. A. Nizhnikovskii, A. V. Fesenko, *Russ. J. Electrochem.* **2006**, *42*, 259.

[8] P. Porion, Y. R. Dougassa, C. Tessier, L. El Ouatani, J. Jacquemin, M. Anouti, *Electrochim. Acta* **2013**, *114*, 95.

[9] D. Bernardi, E. Pawlikowski, J. Newman, *J. Electrochem. Soc.* **1985**, *132*, 5.

[10] R. Srinivasan, A. Carson Baisden, B. G. Carkhuff, M. H. Butler, *J. Power Sources* **2014**, *262*, 93.

[11] Z. Li, J. Zhang, B. Wu, J. Huang, Z. Nie, Y. Sun, F. An, N. Wu, *J. Power Sources* **2013**, *241*, 536.

[12] S. Zhu, J. Han, H.-Y. An, T.-S. Pan, Y.-M. Wei, W.-L. Song, H.-S. Chen, D. Fang, *J. Power Sources* **2020**, *456*, 227981.

[13] J. Fleming, T. Amietszajew, J. Charmet, A. J. Roberts, D. Greenwood, R. Bhagat, *J. of Energy Storage* **2019**, *22*, 36.

[14] M. Guo, G.-H. Kim, R. E. White, *J. Power Sources* **2013**, *240*, 80.

[15] S. Allu, S. Kalnaus, W. Elwasif, S. Simunovic, J. A. Turner, S. Pannala, *J. Power Sources* **2014**, *246*, 876.

[16] D. Werner, A. Loges, D. J. Becker, T. Wetzel, *J. Power Sources* **2017**, *364*, 72.

[17] Y. Zhao, Y. Patel, T. Zhang, G. J. Offer, *J. Electrochem. Soc.* **2018**, *165*, A3169.

[18] I. A. Hunt, Y. Zhao, Y. Patel, J. Offer, *J. Electrochem. Soc.* **2016**, *163*, A1846.

[19] M. Fleckenstein, O. Bohlen, M. A. Roscher, B. Bäker, *J. Power Sources* **2011**, *196*, 4769.

[20] D. Werner, S. Paarmann, A. Wiebelt, T. Wetzel, *Batteries* **2020**, *6*, 13.

[21] D. Werner, S. Paarmann, A. Wiebelt, T. Wetzel, *Batteries* **2020**, *6*, 12.

[22] G. Zhang, C. E. Shaffer, C.-Y. Wang, C. D. Rahn, *J. Electrochem. Soc.* **2013**, *160*, A610.

[23] S. Klink, W. Schuhmann, F. La Mantia, *ChemSusChem* **2014**, *7*, 2159.

[24] P. J. Osswald, S. V. Erhard, J. Wilhelm, H. E. Hoster, A. Jossen, *J. Electrochem. Soc.* **2015**, *162*, A2099.

[25] S. V. Erhard, P. J. Osswald, P. Keil, E. Höffer, M. Haug, A. Noel, J. Wilhelm, B. Rieger, K. Schmidt, S. Kosch, F. M. Kindermann, F. Spingler, H. Kloust, T. Thoennessen, A. Rheinfeld, A. Jossen, *J. Electrochem. Soc.* **2017**, *164*, A6324.

[26] K. Rumpf, A. Rheinfeld, M. Schindler, J. Keil, T. Schua, A. Jossen, *J. Electrochem. Soc.* **2018**, *165*, 2587.

[27] N. Yang, X. Zhang, B. Shang, G. Li, *J. Power Sources* **2016**, *306*, 733.

[28] N. Yang, X. Zhang, G. Li, A. Cai, Y. Xu, *Energy Technol.* **2018**, *6*, 1067.

[29] M. P. Klein, J. W. Park, *J. Electrochem. Soc.* **2017**, *164*, 1893.

[30] R. Korthauer, *Lithium-Ion Batteries: Basics and Applications*, Springer Berlin Heidelberg, Berlin, Heidelberg, **2018**.

[31] C. Pastor-Fernández, T. Bruen, W. D. Widanage, M. A. Gama-Valdez, J. Marco, *J. Power Sources* **2016**, *329*, 574.

[32] *Modern Battery Engineering. A Comprehensive Introduction* (Ed: K. P. Birke), World Scientific, Singapore **2019**.

[33] M. Dubarry, A. Devie, B. Y. Liaw, *J. Power Sources* **2016**, *321*, 36.

[34] G. J. Offer, V. Yufit, D. A. Howey, B. Wu, N. P. Brandon, *J. Power Sources* **2012**, *206*, 383.

[35] X. Gong, R. Xiong, C. C. Mi, *IEEE Trans. Ind. Appl.* **2015**, *51*, 1872.

[36] W. Diao, M. Pecht, T. Liu, *J. of Energy Storage* **2019**, *24*, 100781.

[37] R. Gogoana, M. B. Pinson, M. Z. Bazant, S. E. Sarma, *J. Power Sources* **2014**, *252*, 8.

[38] B. Wang, C. Ji, S. Wang, J. Sun, S. Pan, Du Wang, C. Liang, *Appl. Therm. Eng.* **2020**, *168*, 114831.

[39] X. Liu, W. Ai, M. Naylor Marlow, Y. Patel, B. Wu, *Appl. Energy* **2019**, *248*, 489.

[40] M. Baumann, L. Wildfeuer, S. Rohr, M. Lienkamp, J. of Energy Storage **2018**, *18*, 295.

[41] W. Shi, X. Hu, C. Jin, J. Jiang, Y. Zhang, T. Yip, *J. Power Sources* **2016**, *313*, 198.

[42] G. M. Cavalheiro, T. Iriyama, G. J. Nelson, S. Huang, G. Zhang, *J. Electrochem. Energy Convers. Storage* **2020**, *17*, 021101.

[43] A. Fill, T. Mader, T. Schmidt, R. Llorente, K. P. Birke, *Batteries* **2020**, *6*, 2.

[44] J. Lv, S. Lin, W. Song, M. Chen, Z. Feng, Y. Li, Y. Ding, *Appl. Energy* **2019**, *252*, 113407.

[45] E. Hosseinzadeh, J. Marco, P. Jennings, *J. of Energy Storage* **2019**, *22*, 194.

[46] B. Wu, V. Yufit, M. Marinescu, G. J. Offer, R. F. Martinez-Botas, N. P. Brandon, *J. Power Sources* **2013**, *243*, 544.

[47] O. Schmidt, M. Thomitzek, F. Röder, S. Thiede, C. Herrmann, U. Krewer, *J. Electrochem. Soc.* **2020**, *167*, 60501.

[48] F. An, J. Huang, C. Wang, Z. Li, J. Zhang, S. Wang, P. Li, *J. Storage Mater.* **2016**, *6*, 195.